Tribological behavior of ceramics at high sliding speeds in steam

Hooshang Heshmat and Said Jahanmir*

Mohawk Innovative Technology Inc., Albany, New York 12205, USA

Received 14 December 2003; accepted 25 February 2004

Three sets of tests were conducted using a pin-on-disk tribometer to determine the tribological behavior of ceramics at high sliding speeds in steam. In the first set, the speed was increased from 4000 rpm to 10,000 rpm in 1000 rpm increments. Constant rotational speeds of 4000 rpm, 6000 rpm, 8000 rpm and 10,000 rpm were used in the second test series. In the third series of tests, the rotational speed was slowly increased to 10,000 rpm and allowed to coast down to zero. While the coefficient of friction for silicon nitride/YTZP pair varied between 0.2 and 0.4 without a clear pattern as the speed was increased in the first two test series, it decreased from about 0.6 to 0.2 when the speed was raised to 10,000 rpm in the third test series. This behavior is attributed to the general phenomena of powder lubrication as the wear debris provides an interfacial layer leading to reduced friction at high speeds. The coefficient of friction for silicon nitride/silicon carbide pair was substantially reduced to about 0.02 as the speed was raised. The low coefficient of friction, however, increased to a high level as the speed was further increased. The drop in friction is explained based on analysis of elasto-hydrodynamic lubrication assuming that a water film containing solid particles exists at the interface. Several possible mechanisms are suggested for the transition to a higher friction as the speed is raised: thermal effects at high flash temperatures, low residence times (for water adsorption on surface), collapse of the lubricant film and starvation effects.

KEY WORDS: friction, wear, ceramics, high speed, steam lubrication, silicon nitride, silicon carbide, zirconia

1. Introduction

Steam technology dating back to the 19th century has been effective in both propulsion and power generating systems. They are relatively safe, reliable, and robust, and water is readily available and ecologically sound. As effective as these systems were in early industrialization, they were characterized by low efficiency and large size. New materials and designs may permit the development of high performance machines that break current molds and open up new applications, such as, terrestrial based portable power generating systems, or even energy harvesting systems which take advantage of exhaust steam in fuel cell systems.

Consequently, as smaller machines are developed, new materials introduced, and higher operating speeds and temperatures are employed to achieve the desired higher efficiencies, an in-depth understanding of tribological properties of these new materials will be required. Besides friction characteristics, improved understanding of wear life of these new tribo-material systems is also needed. Under the expected high sliding velocities and potentially high contact stresses, whether for piston engines or steam turbines, wear life and an understanding of the mechanisms present in the wear process will be needed.

There has been a large body of work investigating the tribological characteristics of ceramic/metal and ceramic/ceramic pairs over the years with a variety of lubricants, such as, solid bonded films and even dry powders [1]. Within this body of research, there have been a substantial number of investigations where water is used as a lubricant. These previous studies have provided a solid foundation upon which to build and have identified important surface interactions and mechanisms influencing the friction and wear life of advanced tribo-material systems.

It is a well established that the tribological behavior of material pairs is influenced and to some degree controlled by the nature of surfaces and the films or layers that may form at the interface between the two sliding materials [2]. The types of interfacial films and the properties of these films depend on the chemical nature of the surfaces and the environment present at the interface. Studies of Fisher *et al.* [3–5], Sugita *et al.* [6], Kato *et al.* [7–9] and Jahanmir *et al.* [10–12] have established the role of tribochemical reactions of silicon nitride and silicon carbide ceramics with water. These studies revealed that, for silicon-based ceramics, wear occurs in water (or in presence of environmental water vapor) as a result of tribochemical reaction of the material via the formation of SiO, and its subsequent dissolution in the form of $SiO_2 \cdot xH_2O$ in water or mechanical removal of the hydrated layer in air.

Fischer and Mullins [13] have shown that an amorphous SiO_2 or hydrated SiO_2, film is formed on the wearing surfaces when covalently bonded ceramics (e.g., Si_3N_4 and SiC) slide against each other. As a

*To whom correspondence should be addressed.
E-mail: sjahanmir@mitiheart.com

result, the friction coefficient is reduced. Sasaki [14] also found a hydrated SiO_2 film formed on the worn surfaces when silicon nitride slid against silicon nitride in water. Ajay and Ludema [15] showed that a transfer film forms on wearing surfaces of ceramics with ionic bonds (e.g., Al_2O_3 and ZrO_2) when slid against similar ceramics or steels. This film formation was thought to significantly reduce the wear rate. The studies of Dong and Jahanmir [11,12] have shown that in addition to the tribochemical reactions between ceramics and water, the high contact temperatures cause oxidation reactions and selected diffusion of certain constituents toward the surface leading to formation of mixed transfer layers.

In a pioneering study, Fischer and Tomizawa [16] found that an extremely low coefficient of friction can be obtained for self-mated silicon nitride surfaces in water when the wear scar and the wear track become very smooth by tribochemical wear. They attributed the observed low friction to the possibility of hydrodynamic lubrication by water, even at fairly low speeds of 6 cm/s. Xu *et al.* [17] investigated the dynamic running-in process of silicon nitride sliding in water at sliding speeds ranging from 3 to 12 cm/s and showed that the wear mechanism changed from a mechanical wear process to tribochemically dominated wear as the sliding distance increased. They suggested that for the establishment of hydrodynamic lubrication with water the fluid viscosity should be at least one order of magnitude larger than that of water. They argued that a higher viscosity at the contact may be possible due to the existence of colloidal silica wear particles and the formation of silica layer on friction surfaces.

Chen *et al.* [18] conducted friction and wear studies of self-mated SiC and Si_3N_4 in water and showed that after running-in self-mated Si_3N_4 exhibited lower steady-state friction coefficient than self-mated SiC. This indicated that the chemical response to water of Si_3N_4 and SiC under sliding conditions were different and suggested that the difference in chemical properties, i.e., electronic structure between these two ceramics, affected the observed frictional response. Wong *et al.* [19] confirmed that the low coefficient of friction can be obtained with self-mated silicon nitride and silicon carbide, but not with alumina or zirconia ceramics. It was considered that tribochemical reactions were occurring for Si_3N_4 and SiC, while reaction products did not contribute to the lubrication of Al_2O_3 and ZrO_2. Fischer and Mullins [13] attributed the differences in reaction rates between different ceramics and water to the energy gaps of these materials.

Extensive research has been conducted by Gardos [20] to examine the surface chemistry-induced friction and wear changes with a variety of materials and solid lubricant combinations as a function of atmospheric environment and temperature. Gardos [21] examined the tribochemical changes that occurred with various commercially available α-SiC and diamond coated α-SiC. Tests were conducted on a unique oscillating pin-on-disc tribometer inside a scanning electron microscope. Its primary purpose was to examine the tribological behavior of a variety of materials and solid lubricants, under realistic engineering contact stresses in the MPa to GPa range, as influenced by elevated temperatures in moderate vacuum and in low partial pressures of inert or reactive gases. The coefficient of friction and wear measurements were complemented by surface analyses to evaluate the atomic-level surface interactions by the tribological behavior of microscopic Hertzian contacts. All the friction trends indicated that the changes in adhesion (and thus the coefficient of adhesive friction) could be explained by the number of dangling, reconstructed, or adsorbate-passivated surface bonds on the contacting surfaces as a function of temperature and atmospheric environment.

What is not evident in the information that presently exists in the literature is information that would permit designers to directly identify and select material combinations for steam lubricated engines with a high degree of confidence. A better understanding of the tribological characteristics of advanced materials is needed to continually improve efficiency, reliability and durability of these engine concepts. The objective of this study, therefore, was to determine the tribological behavior of ceramics at high sliding speeds in steam to lay the groundwork of tribological fundamentals for advanced water-lubricated steam engines intended for both mesoscale and macroscale use.

2. Experimental procedure

The ceramic samples selected for testing were silicon nitride (NBD-200), yttria stabilized zirconia (YTZP), and alpha-silicon carbide (α-SiC). Silicon nitride balls were tested against SiC and YTZP disks.

In order to simulate the conditions the materials would experience in a mesoscopic steam engine, the MiTi® high temperature, high-speed tribometer was modified to include a steam generator. A steam can, oven support drip cup, and lower drip cup were machined from stainless steel. To account for the water and water vapor in the system, drain lines were added using stainless steel tubing. The tribometer's spindle was drilled for a drain line and a small drip cup was placed under the spindle. A drain line was also installed in the oven support drip cup. The steam generator was attached to the steam can, and the system was sealed with a silicon sealant. Figure 1 shows the overall set-up for the modified tribometer.

The MiTi® high-speed, high-temperature tribometer has a pin-on-disk configuration and is readily modified to permit ball-on-disk, roller-on-disk or pad-on-disk testing. The tribometer uses a counterbalanced

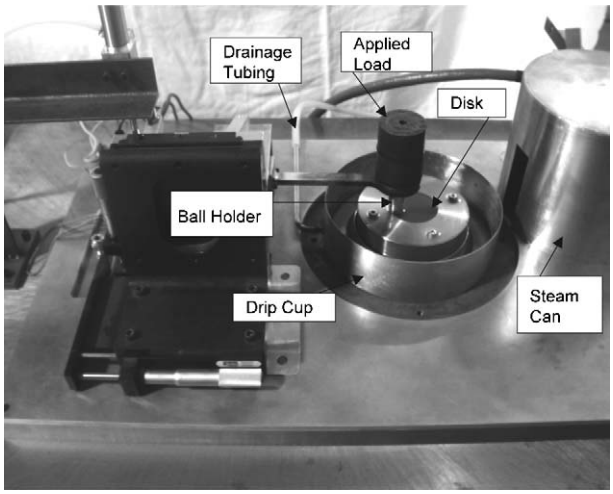

Figure 1. Overall view of the modified MiTi® high-temperature, high-speed, pin-on-disk tribometer.

specimen arm holder that can readily accept a wide range of specimens. A maximum spindle run-out of 5 μm has been demonstrated at speeds to 10,000 rpm. The ability to accept test disks of large diameters, permits multi-track testing on a single specimen at surface speeds up to 60 m/s. A double chamber is used to permit testing in a controlled gas environment at elevated temperatures. The outer chamber may be flooded with purge gas such as nitrogen or argon. The inner chamber is a sealed oven capable of bringing the test environment to 750 °C.

The ball diameter for all samples was 6.35 mm. Due to the differences in disk diameters for the selected materials, the wear track radii were 11 mm for SiC and 17 mm for YTZP, resulting in maximum surface speeds of 11 and 18 m/s. All tests were conducted at a constant applied normal load of 7 N and at speeds up to 10,000 rpm. The tests were run with steam generated at 100 °C at atmospheric pressure. The room temperature and relative humidity were recorded to be 25 °C and 65% respectively. While the balls were used in the as received polished condition, the disks were ground to a surface finish of 50 nm R_a. The temperature inside the chamber and the ball holder temperature were continuously monitored with thermocouples.

Three sets of tests were conducted. In the first set, the speed was increased from 4000 to 10,000 rpm in 1000 rpm increments after 20 s duration at each speed. Constant rotational speeds of 4000, 6000, 8000 and 10,000 rpm were used in the second test series. The total sliding distance in these tests ranged from 5 to 6 km. In the third series of tests, the rotational speed was slowly increased to 10,000 rpm and was held constant for about 20 s. The speed was then allowed to coast down to zero. Each test was repeated at least twice to confirm that the observed results were repeatable. The total wear height of the ball and disk were monitored during the tests with a proximity probe attached to the ball holder. This data was used to estimate the width of the ball wear scar and disk wear track, assuming that the vertical dimensions of the wear scar and the wear track were equal. This information was used to estimate the contact pressure and calculate the lubricant film thickness.

Following the wear tests, the ball wear scar diameter was measured with an optical microspore and the disk wear track width was measured with stylus profilometry. At least three measurements were taken for each wear scar and wear track and the mean and standards deviations were calculated. The widths of the ball wear scars and the disk wear tracks were in most cases equal. However, the wear rates of the disks were much greater than the wear rates of the balls because of the large disk wear track length. Thus, the comparison of wear performance amongst the tribomaterial combinations was made using the wear rate of the disk.

3. Results

As shown in figure 2(a), the effect of speed on the coefficient of friction for the silicon nitride/YTZP pair was erratic. The coefficient of friction varied between 0.2 and 0.4 as the speed was increased from 4000 rpm to 10,000 rpm. A completely different behavior was observed for silicon nitride sliding against silicon

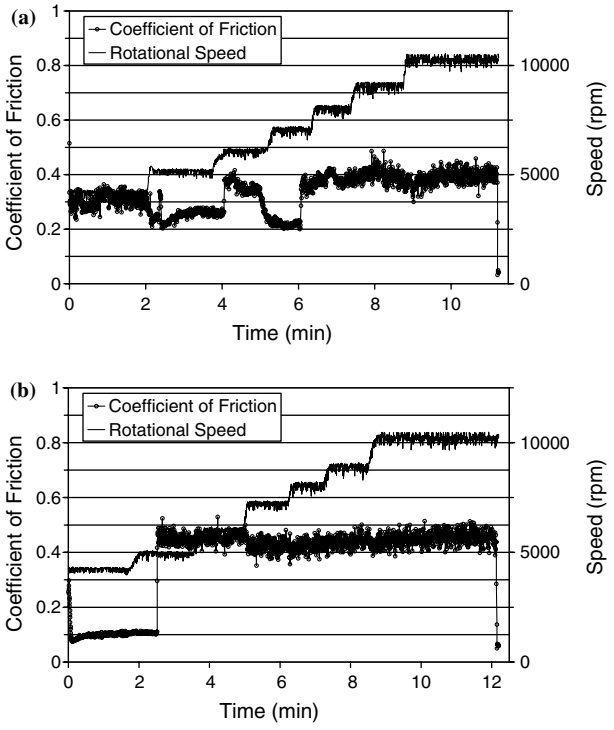

Figure 2. Coefficient of friction as a function of sliding distance in steam as the rotational speed is increased from 4000 to 10,000 rpm; (a) silicon nitride sliding against YTZP and (b) silicon nitride sliding against silicon carbide.

carbide (figure 2(b)). In this case, the coefficient of friction decreased to about 0.1. Then it rapidly increased to about 0.45 sometime after the speed was raised to 5000 rpm. It remained at this value as the speed was further increased to 10,000 rpm.

In constant speed tests, the average coefficient of friction for silicon nitride against YTZP varied between 0.3 and 0.4 as the speed was raised, but the wear rate increased (figure 3(a)). For silicon nitride sliding against silicon carbide, there was no consistent pattern for the wear results, but the average coefficient of friction was reduced from 0.40 to 0.15 (figure 3(b)). Inspection of the friction–time plots for these tests, showed that the coefficient of friction was initially less that 0.1, but it rapidly increased to 0.5 half way through the testing period (figure 4). Therefore, the average values plotted in figure 3(b) do not show that a low value was attained at the beginning of sliding. As shown in figure 4, the ball holder temperature increased soon after the coefficient of friction increased to 0.5.

In the third test series in which the rotational speed was raised to 10,000 rpm followed by coast down, the coefficient of friction for silicon nitride sliding against YTZP initially increased from 0.30 to 0.56 (figure 5(a)). This was followed by a decrease to 0.2 as speed approached 10,000 rpm. As coast-down began the coefficient of friction steadily increased to nearly 0.8. In these tests a new ball and a new disk track region were used. Several of the tests were repeated

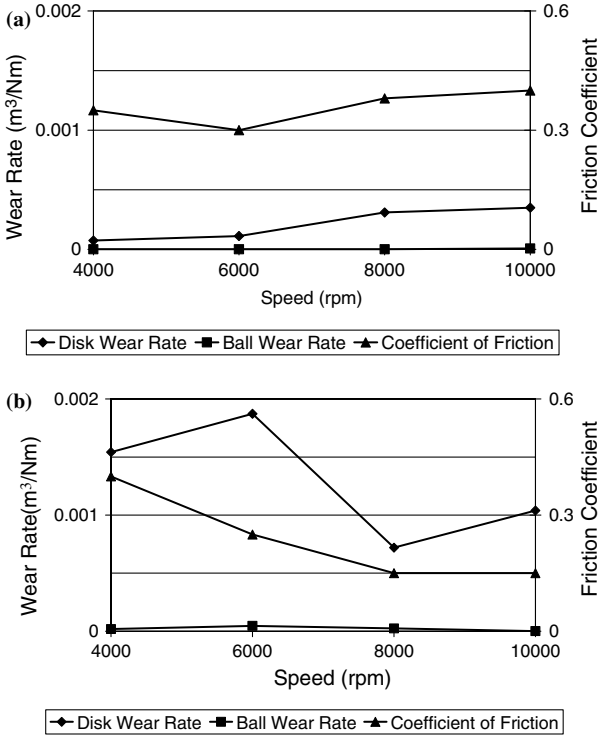

Figure 3. Coefficient of friction and wear rates in steam as a function of speed in constant speed tests; (a) silicon nitride sliding against YTZP and (b) silicon nitride sliding against silicon carbide.

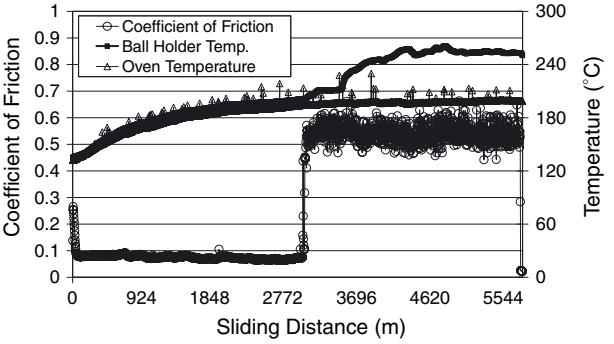

Figure 4. Friction-time trace for silicon nitride sliding against silicon carbide at 4000 rpm in steam.

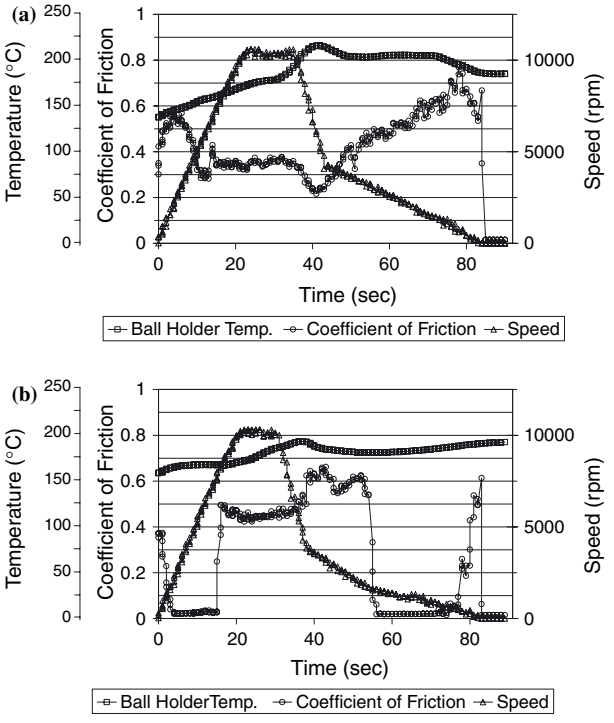

Figure 5. Coefficient of friction in steam as a function of time for the tests in which the speed was raised to 10,000 rpm followed by coast down; (a) silicon nitride sliding against YTZP and (b) silicon nitride sliding against silicon carbide.

with the same worn balls on the worn tracks. The resulting coefficient of friction was very similar to the results obtained with new balls and tracks.

The coefficient of friction for silicon nitride sliding against silicon carbide showed a distinct behavior (figure 5(b)). The coefficient of friction was initially high at about 0.4 and as the speed was raised to 2000 rpm the coefficient of friction rapidly decreased to 0.02. This was followed by a sharp increase to 0.5 as the speed approached 8000 rpm. At the start of coast down there was another increase in the coefficient of friction to 0.65. As coast down continued to 2000 rpm the coefficient of friction decreased again to about 0.02. Upon further decrease in speed to 500 rpm the coeffi-

cient of friction rose to 0.6. When the test on silicon nitride/silicon carbide pair was repeated under dry conditions (i.e., without steam), the frictional characteristics were significantly different. Initially, the coefficient of friction increased to 0.65 as the speed was raised, figure 6. This increase was followed a gradual reduction in the coefficient of friction to 0.45. During coast down the coefficient of friction gradually increased to 0.8. This behavior is similar to that observed for silicon nitride/YTZP pair tested in steam (figure 5(a)). The repeat tests for all three material pairs showed repeatable trends, similar to those presented here.

4. Discussion

The results of this study have shown that the coefficient of friction for silicon nitride/YTZP pair in steam as well as for silicon nitride/silicon carbide pair in air decrease with increasing speed. This behavior may be attributed to the general phenomena of powder lubrication (figure 7). The wear debris that is generated, i.e., the third body, forms an interfacial layer between the two sliding pairs. The third body layer is subjected to shear flow, which helps support the load and reduce the overall coefficient of friction [22]. It is however, not possible a priori to predict the value of the coefficient of friction, since it would depend on the size and morphology of the wear debris, the presence or absence of products of tribochemical reactions (i.e., oxides and hydroxides) and of course the chemical nature of the entire third body material. It is, however, interesting to note that the minimum coefficient of friction for the aforementioned pairs in steam is lower than the silicon nitride/silicon carbide pair in air. The lower friction in steam may be a result of reduced shear resistance of the third body due the presence of water molecules or droplets. Figure 8 clearly depicts an overall summary of the weights of the two components in a tribological film: A—Effects that are produced in a *lubricant* by the relative motion of the tribosurfaces (*Lubricant* is defined as any third-body

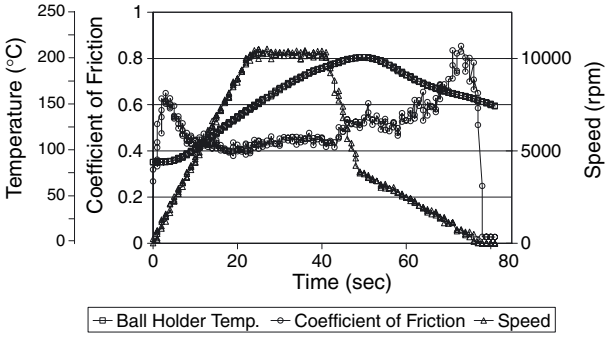

Figure 6. Coefficient of friction for silicon nitride sliding against silicon carbide in air (without steam) as a function of time for the tests in which the speed was raised to 10,000 rpm followed by coast down.

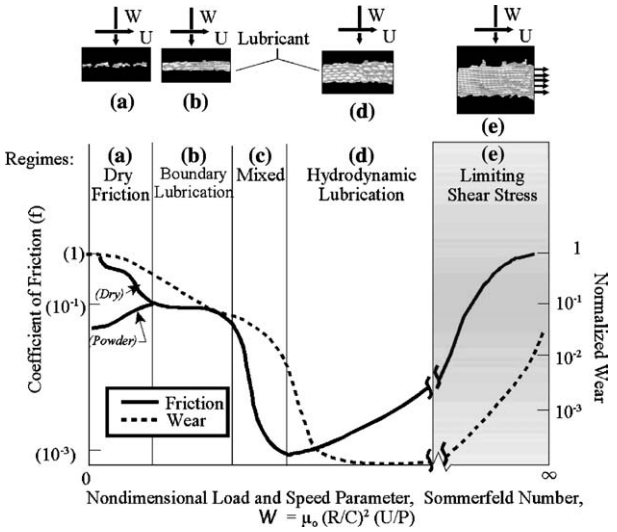

Figure 7. Extended Stribeck curve for powder lubrication (from References 26, 27).

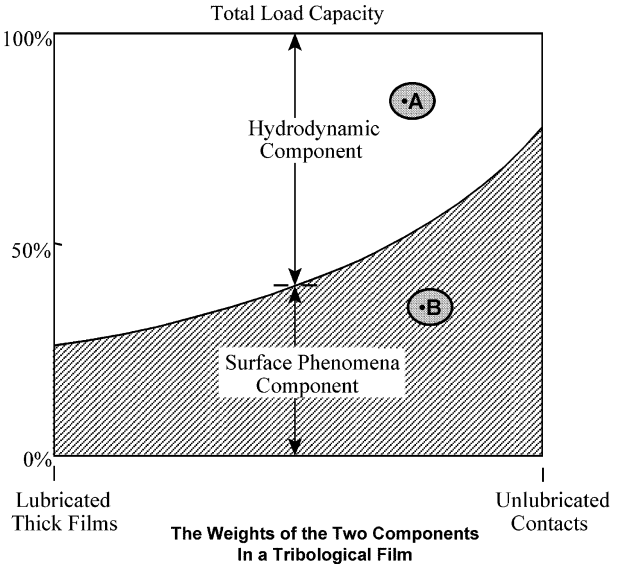

Figure 8. Summary of the weights of two components in a tribological film (from References 26, 27). A—Effects that are produced in a *lubricant* by the relative motion of the tribosurfaces. B—Effects due to the elastic, plastic, chemical, molecular, and other surface phenomena in the zone of interface contact.

located in the clearance that is not integral with either surface) and B—Effects due to the elastic, plastic, chemical, molecular and other surface phenomena in the zone of interface contact. The second observation in this study was the unique behavior of the silicon nitride/silicon carbide pair in steam. The coefficient of friction in that case was substantially reduced to about 0.02 as the speed was raised. The coefficient of friction, however, increased to a high level as the speed was further increased. The drop in friction may be explained based on suggestions made by Tomizawa and Fischer [16] and/or Kato *et al.* [17]. According to

Tomizawas and Fisher [16] friction is reduced because of the formation of extremely smooth wear flats through tribochemical wear and initiation of hydrodynamic lubrication with water. Kato *et al.* [17], however, attribute the low friction to the presence of a viscous interfacial layer consisting of water and products of tribochemical reaction between water and the silicon based ceramics (i.e., silica gel) in either case, one should expect a speed-dependant phenomena. All published results by Fischer and Kato and their coworkers have been conducted at speeds much lower than those used in our study. Therefore, they did not observe the transition to a higher friction as the speed was raised. Such an increase may be due to several factors including high flash temperatures, low residence times (for water adsorption on surface), collapse of the lubricant film, starvation effects and others. The following analysis was conducted to gain an understanding of the observed frictional transitions.

The lubricant film thickness was estimated for a test conducted with a silicon nitride/silicon carbide pair as the speed was raised to 10,000 rpm and allowed to coast down to rest (e.g., see figure 5(b)). Commonly used equations for EHD lubrication [23] and Hertzian contact pressure calculations were employed. The input parameters were the viscosity of steam, elastic properties of the tribo-pairs, sliding speed, contact temperature, contact load, and contact geometry (i.e., radii of curvature for the ball and the disk, and wear scar dimensions for equal time intervals during the test estimated from the data collected with the proximity probe). First, the elastically deformed shape of the contact was calculated. Since all the geometric parameters were not known (e.g., the radii of curvature inside the wear tracks), an assumed value was used and the calculations were performed iteratively until contact dimensions became equal to the measured wear scar and wear track size. The computational perturbations about the geometric data continued until the calculated values of the traction force approached the experimentally measured values of friction force. Once convergence was reached, the calculated values of contact pressure and film thickness were assumed to correspond to the experimental condition employed in the calculations.

In order to estimate the viscosity of water/steam at the contact interface, it was assumed that the fluid at the interface contained 20% by volume solid particles, and the slurry viscosity was calculated using the following equation [24,25]:

$$\ln \mu_{\mathrm{R}} = (2.5N + 2.7N^2)/(1 - 0.61N),$$

where μ_{R} is the relative viscosity and N is the solid fraction. Note that the relative viscosity, assuming that the reference viscosity in the absence of particles is unity, increases exponentially. The reference viscosity of water/steam corresponding to the contact temperature and pressure for each particular test condition was obtained from appropriate published data. The contact temperature was assumed to be the same as the measured ball holder temperature. Obviously this assumption would introduce a systematic error since the actual contact temperature is expected to be larger than the ball holder temperature. Since our intention is to establish a trend for the lubricant film thickness, rather than calculate the exact value, this assumption may be acceptable.

The calculated EHD lubricant film thickness and the traction coefficients (coefficient of friction) for equal time intervals are plotted in figure 9 as a function of a non-dimensional load and speed parameter. This parameter, which is a modified Sommerfeld number and is used in the extended Stribeck curve is defined as [26,27]:

$$W = \frac{\mu_0 \bar{U}(1/R)(R_{\mathrm{o}}/R_{\mathrm{a}})^2}{P_{\max}}$$

where μ_{o} is the reference viscosity, $\bar{U}$ is the effective speed, R the radius of wear track on disk, R_{o} the radius of ball, R_{a} the surface finish of ball and $P_{\max}$ is the maximum contact pressure.

Figure 9(a) and (b) shows the experimental coefficients of friction, and calculated film thickness and maximum Hertzian pressure as a function of non-dimensional load and speed parameter for silicon nitride sliding against silicon carbide in steam, for speeds up to 10,000 rpm (figure 9(a)) and coast down (figure 9(b)). Figure 9(a) shows that initially the contact pressure drops rapidly and the coefficient of friction is reduced as the rotational speed is increased. The drop in contact pressure is due to initial rapid wear rate. The contact pressure then gradually decreases and the lubricant film thickness slowly increases as the speed is increased. Note that the film thickness continues to increase even after the coefficient of friction increases sharply. The film thickness is on the order of 3–7 μm when the coefficient of friction is at it lowest value. Although such a relatively thick lubricant film as compared to the initial ball and disk roughness would indicate full fluid film lubrication, the calculated values may not be accurate due to the simplifying assumptions made for these calculations. Nevertheless, these results indicate that fluid film lubrication may be possible. It is important to point out that the state of the fluid at the interface is very complex. The viscosity might increase due to local dissolution of tribochemical reaction products and the powder lubrication effects due to undissolved wear particles (e.g., figure 8). A low wear rate and concomitant small reduction in contact pressure, when the friction is rising, implies an increase in film stiffness since the film thickness is increasing. This may cause a drop in viscosity because of pressure–viscosity effects and reduce the frictional force.

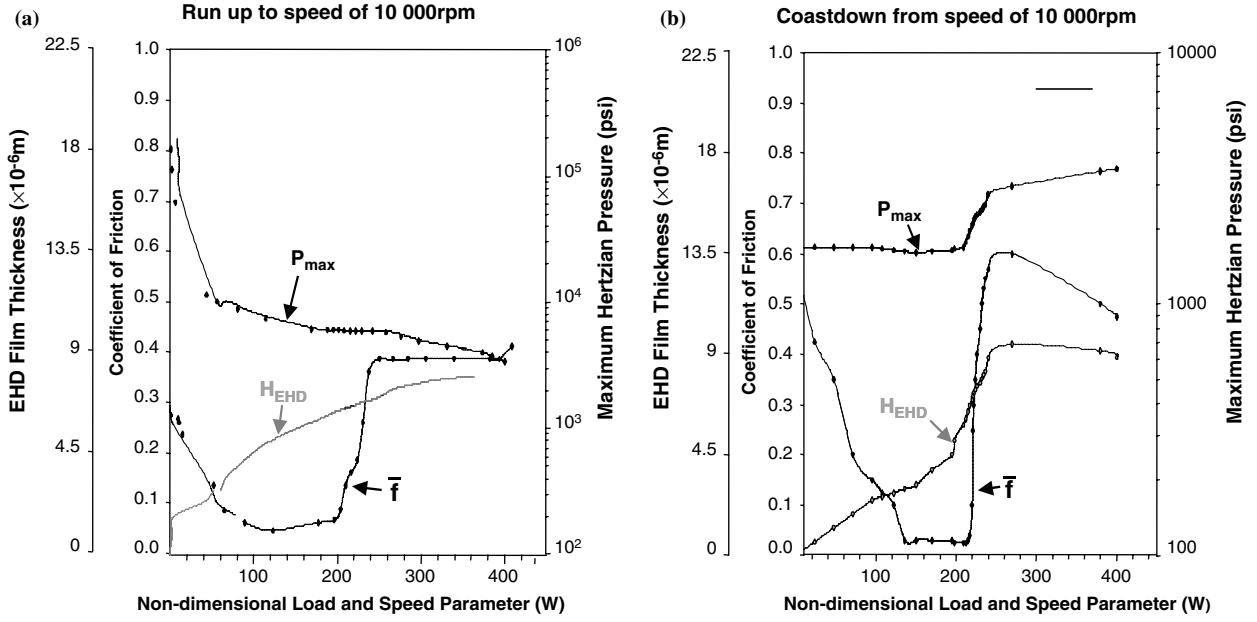

Figure 9. Calculated EHD film thickness as a function of non-dimensional load and speed parameter for silicon nitride sliding against silicon carbide in steam. The calculated values of maximum contact pressure and the coefficients of friction from experiments are also included in the graphs.

As the sliding speed decreases, during coast down (figure 9(b)), the film thickness gradually decreases while the coefficient of friction is reduced again. The film thickness value during the second drop in friction is in the same range as those during the first drop. Upon further decrease in speed, film thickness approaches zero.

The rise in friction figure 9(a), as the speed is increased, is possibly due to thermal effects or lubricant starvation, since the calculated film thickness continues to increase. During starvation, which has been observed for lubrication with powders and liquid lubricants [28] the coefficient of friction rapidly increases [29] when the starvation index drops below 20%. The required fluid flow through the interface to form a complete EHD film may not be fully satisfied. The greater the surface velocity, greater is the need for lubricant flow. The moving surface must drag a large amount of steam into the contact and reduce it to liquid water under the contact pressure. There is a possibility for discontinuity, thus a mixture of liquid and vapor enter the contact leading to a two-phase flow condition. Such a situation maybe considered as fluid film starvation. There is a threshold in the starvation where friction starts to increase. However, the starvation effect was not included in the EHD analysis presented here.

It should be pointed out here that possible effects on tribological behavior of corrosive agents and high temperatures and pressures in steam engines cannot be ignored. The possible influence of carbonic acid corrosion and amines, often used to prevent corrosion, on tribological behavior of the selected materials, e.g., ceramics, should be investigated.

The steam temperature in the present study was about 100 °C at ambient pressure. This is much lower than the anticipated steam temperature and pressures in steam engines. In order to obtain tribological data under relevant set of operating conditions, one must conduct the friction tests at high temperatures and pressures. Unfortunately, this task must await the development of a new tribometer that can be used under such extreme environments. We are presently developing a high-temperature, high-pressure, tribometer for such studies. The results will be reported in due course.

4. Conclusions

The following conclusions are drawn from the study on steam lubrication of ceramics presented in this paper:

1. The effect of speed on the coefficient of friction of silicon nitride against YTZP was erratic and varied between 0.2 and 0.4 as the speed was increased incrementally from 4000 to 10,000 rpm. A completely different behavior was observed for silicon nitride sliding against silicon carbide. The coefficient of friction decreased to about 0.1. Then it rapidly increased to about 0.45 sometime after the speed was raised to 5000 rpm.
2. The average coefficient of friction for silicon nitride against YTZP varied between 0.3 and 0.4 as the speed was raised from 4000 to 10,000 rpm in

constant speed tests, but the wear rate increased. For silicon nitride sliding against silicon carbide, there was no consistent pattern for the wear results, and the average coefficient of friction was reduced from 0.40 to 0.15. In these tests the coefficient friction was initially less that 0.1, but it rapidly increased to 0.5 half way through the testing period.

3. The coefficient of friction for silicon nitride/YTZP pair in steam, as well as for silicon nitride/silicon carbide pair in air decreased with increasing speed. This behavior may be attributed to the general phenomena of powder lubrication.
4. The coefficient of friction for silicon nitride/silicon carbide pair in steam was substantially reduced to about 0.02 as the speed was raised. The coefficient of friction, however, increased to a high level as the speed was further increased. The drop in friction is explained based on analysis of elasto-hydrodynamic lubrication assuming that steam is reduced to water under contact pressure and a water film containing solid particulates exists at the interface. Several possible mechanisms are suggested for the transition to a higher friction as the speed is raised: thermal effects at high flash temperatures, low residence times (for water adsorption on surface), collapse of the lubricant film, and starvation effects.

Acknowledgments

The support received from DARPA and AFOSR are gratefully acknowledged. We thank Lt. Captain Trulove of AFOSR for his sustained interest in Tribology. The technical assistance provided by Dave Slezak of MiTi and Sara Atwood (Summer student) is appreciated. We dedicate this paper to our late friend Mike Gardos of DARPA, who made tremendous contribution to Tribology.

References

[1] H. Heshmat, Lubrication Engineering, 49 (1993) 791–797.
[2] H. Heshmat, M. Godet and Y. Berthier, Lubrication Engineering 51 (1995) 557–564.
[3] H. Tomizawa and T.E. Fischer, ASLE Trans. 29 (1986) 481–488.
[4] T.E. Fischer and H. Tomizawa, Wear 105 (1985), 29.
[5] T.E. Fischer and H. Tomizawa, J. Vac. Technol. A 6 (1986) 3027.
[6] T. Sugita, K. Ueda and Y. Kanemura, Wear 97 (1984) 1–8.
[7] K. Kato and K. Adachi, Wear 253 (2002) 1097–1104.
[8] M. Chen, K. Kato and K. Adachi, Tribol. Int. 35 (2002) 129–135.
[9] J. Xu and K. Kato, Wear 245 (2000) 61–75.
[10] Jahanmir, S and T.E. Fischer, STLE Trans. 31 (1987) 32–43.
[11] X. Dong and S. Jahanmir, Wear 165 (1993) 169–180.
[12] X. Dong and S. Jahanmir, Tribol. Int. 28 (1995) 559–572.
[13] T.E. Fischer and W.M. Mullins, J. Phys. Chem. 96 (1992) 5690–5701.
[14] S. Sasaki, "The Effects of Surrounding Atmosphere on the Friction and Wear of Alumina, Zirconia, Silicon Carbide and Silicon Nitride," K.C. Ludema ed. Proc. Int. Conf. On Wear of Materials (1989) 409–417.
[15] O.O. Ajai and K.C. Ludema, "Formation of Transfer Film During Ceramics/Ceramics Repeat Pass Sliding," K.C. Ludema, ed. Proc. Int. Conf. on Wear of Materials (1989) 349–359.
[16] H. Tomizawa and T.E. Fischer, ASLE Trans., 30 (1987) 41–46.
[17] J. Xu, K. Kato and T. Hirayama, Wear 205 (1997) 55–63.
[18] M. Chen, K. Kato and K. Adachi, Tribol. Let. 11 (2001) 23–28.
[19] H-C. Wong, N. Umehara and K. Kato, Tribol. Let. 5 (1998) 303–308.
[20] M.N. Gardos *"Tribology Research: From Model Experiment to Industrial Problem,"* G. Dalmaz, et al. ed. (2001) 253.
[21] M.N. Gardos, "Fundamentals of Tribology and Bridging the Gap between Macro- and Micro/Nanoscales," B. Bhushan, ed. NATO SCI. Ser. II, 503, (Kluwer Academic Publishers, Dordrecht) (2001).
[22] H. Heshmat, O. Pinkus and M. Godet, STLE Trans. 32 (1989) 32–41.
[23] J. Wolowit and J. Anno, Modern Developments in Lubrication Mechanics, Applied Science, 1977.
[24] A. Einstein, Annalen der Physik 19 (1906) 289–306.
[25] J. Vand, J. Phys. Colloid Chem., 52 (1968) 277.
[26] H. Heshmat, Tribol. Trans. 38 (1995) 269–276.
[27] H. Heshmat, Proceedings of the 20th Leeds-Lyon Symposium on Dissipative Processes in Tribology, Lyon, France, September 7–10, 1993. Elsevier, Tribology D. Dowson, ed. Series 27 (1994) 45–64.
[28] H. Heshmat, Wear 162–164 (1993) 518–528.
[29] H. Heshmat, A. Artiles and O. Pinkus, *The Proceedings of the 13th Leeds-Lyon Tribology Symposium, Leeds, UK, September 1986*. Tribology Series 11, D. Dowson, ed. (Elsevier, Amsterdam, 1986) p. IV(ii).